Aerospace Science and Technology 55 (2016) 24–33

Contents lists available at ScienceDirect

Aerospace Science and Technology

www.elsevier.com/locate/aescte

Aerodynamic shape optimization for minimum robust drag and lift reliability constraint

Dimitrios I. Papadimitriou *, Costas Papadimitriou

Department of Mechanical Engineering, University of Thessaly, Pedion Areos, Volos 38334, Greece

ARTICLE INFO

Article history:
Received 8 November 2015
Received in revised form 23 April 2016
Accepted 4 May 2016
Available online 9 May 2016

Keywords:
Aerodynamic shape optimization
Robustness
Reliability
FORM
Sparse grid quadrature
Adjoint method

ABSTRACT

A methodology for shape optimization of aerodynamic bodies under uncertainties is presented. Flow-related and geometrical uncertainties are considered and quantified by probability distribution functions. The optimal shape is computed by minimizing a robust estimate of the drag coefficient subject to reliability constraint for the lift coefficient. The robust drag is formulated as a weighted sum of the mean and the standard deviation of the drag coefficient over the space of uncertain parameters. The mean and standard deviation of the drag coefficient are computed using sparse grid techniques. The lift reliability, defined by the probability the lift coefficient is lower than a reference value, is computed using First Order Reliability Method (FORM). A gradient-based optimization algorithm is used to obtain the optimal shape. The sensitivity derivatives of robust drag measure and the lift reliability with respect to the shape controlling and flow related design parameters as well as the uncertain parameters are computed using the adjoint problem for the flow. The methodology is applied to pure aerodynamic shape optimization, comparing optimal designs that arise from the formulation to optimal designs that correspond to special cases, including the case of no uncertainties. A 2D airfoil case is designed based on the Euler equations under uncertain Mach number and angle of attack and geometric variability.

1. Introduction

The availability of powerful Computational Fluid Dynamics (CFD) models has allowed the scientific community to investigate and develop a variety of algorithms applied to shape optimization, optimal active flow control with suction-blowing jets, topology optimization, etc. However, the resulting optimal design lacks good performance when the values of some parameters of the problem are uncertain or may vary within a range. Optimal designs based on a single value of the models parameters are very sensitive to uncertainties in the parameters in the sense that the performance deteriorates considerably in the neighborhood region where the parameters are likely to take values. Thus, the optimal design should take into account the variability or uncertainties of such parameters [51,50,46,45] by minimizing an overall measure of the performance over all possible values of the uncertain parameters and the sensitivity of performance to uncertainties. A multi-point optimization approach has been introduced to account for uncertainties by computing the performance in multiple points in the uncertain parameter space [34,16,23,35].

Probability distribution functions (PDFs) are often used to quantify uncertainties in simulations and probability calculus is applied to propagate the uncertainties in output quantities of interest (QoI). In design optimization the output QoI are associated with system performance measures involved in the objective function or the constraints. The mean and standard deviation are conveniently used as simple measures of uncertainty in QoI. Thus, the obvious choice in design optimization under uncertainties would be to minimize the mean value of the performance function and the standard deviation over the range of possible values of these uncertain parameters [39,41].

The mean and standard deviation are formulated as multi-dimensional integrals in the uncertain parameter space. The computation of these multidimensional integrals may be based on deterministic or stochastic approaches, including derivative-based, sampling and grid-based approaches. The derivative-based robust design uses a Taylor or asymptotic expansion and the multi-dimensional integrals are approximated by expressions that involve the first and second derivative of the performance variables with respect to the uncertain parameters [39,41,42,27,36]. Such approaches are quite fast, but lack accuracy in cases of large uncertainties, or in cases where the linearization of the performance function in the uncertain parameter space is not adequate such as in the case of transonic flow.

* Corresponding author. Tel.: +30 24210 74006.
E-mail addresses: dpapadim@uth.gr (D.I. Papadimitriou), costasp@uth.gr (C. Papadimitriou).

http://dx.doi.org/10.1016/j.ast.2016.05.005
1270-9638/

Stochastic approaches for the estimation of the statistical moments are usually based on advanced Monte-Carlo (MC) methods [27,49,19] which are costly due to the very large number of analyses on the sample points required to compute these integrals. In addition, the sample estimates of the integrals are non-smooth functions of the design variables due to the variability of the samples between design points, complicating the use of gradient-based optimization algorithms over the uncertain parameter space. The grid-based approaches [8] are more accurate for the estimation of the uncertainties but they usually require a large number of CFD evaluations on the predefined grid nodes. The sparse-grid approach [47,14,5] is a remedy to the numerous required evaluations, substantially reducing the number of grid points and thus the computational cost in relation to grid-based and Gauss quadrature techniques. Using grid-based techniques, the multi-dimensional integrals for the mean and standard deviation become smooth functions of the design variables.

Uncertainties should also be taken into account for the estimation of the constraints involved in design optimization. The constraints should be satisfied for all possible values of the uncertain model parameters, an implementation that is not practical to carry out in most problems. Using PDF to quantify uncertainties and taking into account that the performance objective competes with the constraints, the requirement to satisfy the constraint at all possible values of the model parameters, even the values with relatively small plausibility based on the assigned PDF, results in significant deterioration of the system performance. In [45] for problems of shape optimization under uncertainty in CFD, the constraints are satisfied in the grid points used to approximate the multi-dimensional integrals involved in the robust performance measure. The drawback of this approach is that it fails to provide an overall measure of constrained violation over the parameter space. An alternative rational approach is to require that the constraint not to be violated with a given probability, formulating the constraint in terms of a reliability or, its complement, the probability of unacceptable performance. First-order reliability methods (FORM) [10,9] are most often used to approximate the resulting multi-dimensional reliability integrals over the domain in the uncertain parameter case where the performance criteria for the constraint are violated [28,30,21,13].

The optimal design under uncertainties is often formulated as a problem of minimizing a weighted average of the mean value and standard deviation of a performance function subject to the reliability constraints expressed in terms of the probability of unacceptable performance is lower than a small given probability value. In structural mechanics problems, the formulation has been applied for sizing, shape and topology optimization [30,20,17]. In CFD, the design optimization under uncertainties with reliability constraints may be found in the literature, almost exclusively for problems related with structural constraints in reliability-based aerostructural optimization problems. In [32], the wing mass and lift over drag ratio is minimized subject to probabilistic constraints on structural stresses using the FORM methodology. [11] applies a support vector machine method for the minimization of the probability of failure in stability (flutter) aeroelastic problems. The only flow related reliability-based shape optimization where the probability that the lift to drag ratio is lower than a given value, is computed and minimized may be found in [1], where the constraint is defined by the probability that the maximum stress exceeds another given threshold. The uncertain parameters are the angle of attack and the thickness of the wing plate and FORM is used to evaluate the reliability integral with respect to the two uncertain parameters.

This study presents a methodology for shape optimization of aerodynamic bodies by minimizing a robust measure of the drag coefficient under reliability constraint on the lift coefficient. The objective function is formulated as a weighted sum of the mean and the standard deviation of the drag coefficient. Minimizing the mean assures the smallest possible drag, while minimizing the standard deviation assures an optimal design corresponding to a drag value that is the least sensitive to parameter uncertainties. The sparse grid method is used to compute the mean and the standard deviation of the drag coefficient values at the grid points in the parameter space. The sparse grid approach based on different PDFs can be considered as a multipoint approach, although the sparse grid differs from the multipoint approaches [24] on the selection of the grid points to be consistent with the underline PDF and convenient to efficiently compute the statistical moments of the output quantities of interest. One of the contributions of this work is to impose the aerodynamic constraints on the lift coefficient in a probabilistic manner, requiring that the probability the lift coefficient is less than a reference value, denoted here as the probability of unacceptable performance, be bounded by a small user-defined probability. The FORM is used to estimate the probability of unacceptable performance or “failure” probability using the design point in the parameter space. A gradient-based approach is used to solve the constraint optimization problem. The adjoint approach for the underlining flow is applied for the computation of the first-order derivatives of the mean and the standard deviation as well as the probability of unacceptable performance with respect to the shape controlling parameters and the uncertain parameters, making the computation of sensitivities independent of the number of design variables and uncertain parameters.

The method is applied to the robust optimization of the shape of the RAE 2822 airfoil, the aerodynamic optimization of which has been presented in [45,22,6]. The shape is parameterized using Bézier control points [25]. The coordinates of these control points as well as the mean value of the angle of attack are considered as the design parameters to be optimized. The uncertainties considered are the values of the Mach number and the angle of attack as well as the geometrical uncertainties. Unlike existing geometry parameterization and uncertainty quantification schemes, in the present work the geometric variability is modeled by postulating PDFs to quantify uncertainties in the location of the control points. The proposed design optimization framework under uncertainties is illustrated for a 2D transonic flow governed by the Euler equations. The modeling using the Euler equations is for demonstration purposes, since the inviscid model does not always yield physically significant results [26]. The method of moving asymptotes (MMA) algorithm [48] is used to solve the constrained optimization problem. The importance of considering uncertainties, the effect of the type and magnitude of uncertainties, as well as the effect of the bound on the lift coefficient probability in the optimal design is investigated. The formulation for the robust aerodynamic optimization, minimizing a robust measure of the drag coefficient, under a reliability-based aerodynamic constraint imposed on the lift coefficient, constitutes the main contribution of this paper. The performance of the proposed robust drag optimization under lift reliability constraint is evaluated by comparing results with the ones obtained from the sole robust optimization, sole reliability-based optimization and deterministic optimization.

2. Aerodynamic shape optimization

2.1. Formulation of shape optimization neglecting uncertainties

In deterministic aerodynamic optimization the objective function to be minimized is usually the drag coefficient $C_D(\boldsymbol{\rho})$ constrained by the lift coefficient $C_L(\boldsymbol{\rho})$ not to exceed a predefined value, where $\boldsymbol{\rho} = (\boldsymbol{\rho}_g, \boldsymbol{\rho}_f)$ are the design variables, i.e. the geometrical variables $\boldsymbol{\rho}_g$ controlling the shape of the aerodynamic

body such as the shape of an airfoil as well as flow related variables $\boldsymbol{\rho}_f$ such as the angle of attack. The constrained optimization problem is defined as [23,46]

$$\min_{\boldsymbol{\rho}} \quad C_D(\boldsymbol{\rho}) \tag{1a}$$

$$s.t. \quad C_L(\boldsymbol{\rho}) \geq C_{L,ref} \tag{1b}$$

where the drag coefficient C_D and lift coefficient C_L are given by

$$C_D = \frac{D}{\frac{1}{2}\bar{\rho}\bar{v}^2 A}, \quad C_L = \frac{L}{\frac{1}{2}\bar{\rho}\bar{v}^2 A} \tag{2}$$

with the drag D and lift forces L defined by the integrals over the airfoil contour S from the expressions

$$D = \int_S p n_i k_i dS, \quad L = \int_S p n_i l_i dS \tag{3}$$

Also, p is the pressure value, n_i are the components of the normal unit vector pointing toward the airfoil, k_i and l_i are the components of the unit vector normal and parallel to the far-field velocity $\bar{v}$, respectively, $\bar{\rho}$ is the far-field density and A is the airfoil chord.

The geometrical design variables $\boldsymbol{\rho}_g$ included in $\boldsymbol{\rho}$ consist of either the wall boundary nodes of the computational grid or the control point coordinates of a parameterization scheme [43,37]. In the former case, a smoothing function should be employed in order to certify that the obtained aerodynamic geometry is smooth [43]. In the case of a parameterization scheme [37], the parameterization functions make sure that the geometry is smooth. In this study, the Bézier parameterization [25] has been employed and the design parameter vector $\boldsymbol{\rho}_g$ contains the (x, y) coordinates of the Bézier control points that parameterize the aerodynamic shape. Also, the mean value of the angle of attack is considered as a design variable $\boldsymbol{\rho}_f$ to be optimized mainly to control the lift related constraint.

2.2. Modeling of uncertainties

In aerodynamic shape optimization the most important uncertainties are the flow related ones, arising from the different range of operation conditions related to the Mach number and angle of attack, as well as Reynolds number for a viscous flow modeled by the Navier–Stokes equations. Geometrical uncertainties due to lack of knowledge of the exact geometry of the aerodynamic shape owing to manufacturing imprecision, etc., are also important and should be considered. In the case of using a RANS turbulence models, the values of the parameters of the model should be considered as uncertain and handled together with the flow related and geometrical uncertainties. Last but not least, are the uncertainties associated with the values of the medium properties such as viscosity and density.

Optimal designs based on nominal values of the model parameters lack robustness to variations in the nominal values. The optimal shape should be designed to be insensitive to variations in the values of the model parameters that may result either from the different operation conditions on the Mach and angle of attack, manufacturing variability in the airfoil shape, etc. The objective of the design optimization under uncertainties is to estimate the optimal shape that is robust to uncertainties in the parameter values, meeting at the same time the lift constraints for all possible values of the uncertain model parameters.

Parameter uncertainties are quantified by PDFs and spatially varying uncertainties are quantified by random fields. The vector $\boldsymbol{\theta}$ is introduced to contain the uncertain parameters related to the flow conditions, such as Mach, angle of attack and Reynolds number, the medium properties such as viscosity and density, as well as other parameters associate for example with the RANS turbulence models. The uncertainties in these parameters are quantified by assigning a PDF $p(\boldsymbol{\theta})$ over the domain (support) of variation of these parameters, quantifying how plausible is each possible value of these parameters. For a number of parameters in $\boldsymbol{\theta}$, such as Mach, Reynolds number and angle of attack, the uncertainties are usually postulated to be representative of the variability expected during operation based on engineering judgment. For other parameters, such as the turbulence model parameters, the uncertainties can be quantified by experimental measurements using for instance Bayesian techniques [40,2,33,7,12].

The spatial uncertain variability of the airfoil shape is often quantified by random fields [45] which can be discretized using Karhunen–Loève [15] and represented by a set of random variables. The inclusion of geometrical uncertainties in the aerodynamic shape optimization procedure has been presented in [45] without, however, dealing with reliability constraints. Using Bézier control points to parameterize the airfoil suction and pressure sides through the Bernstein polynomials, the uncertain parameters are the coordinates (x, y) of the control points. At the same time these coordinates are part of the design parameters $\boldsymbol{\rho}$ to be optimized. Thus, the spatial distribution of geometric uncertainties is modeled through the uncertainties in the location $\boldsymbol{\rho}_g$ of the control points. Specifically, the uncertainty in the spatial distribution of the geometrical control parameters $\boldsymbol{\rho}_g$ is quantified by a random vector $\tilde{\boldsymbol{\rho}}_g$ such that

$$\tilde{\boldsymbol{\rho}}_g = \boldsymbol{\rho}_g + \boldsymbol{\eta} \tag{4}$$

where $\boldsymbol{\eta}$ is considered to be a zero-mean Gaussian random vector with covariance Σ selected to quantify the uncertainty of the design variables about their mean value $\boldsymbol{\rho}_g$. To account for correlation in the uncertainty between control points, the covariance matrix is chosen to be non-diagonal. Herein, an exponentially decaying spatial correlation structure is assumed so that the (i, j) component is given by $\Sigma_{ij} = \sigma^2 exp\left(-\frac{r_{ij}}{\lambda}\right)$, where σ and λ are the user defined standard deviation and spatial correlation length, and r_{ij} is a measure of the distance between the control points i and j. The zero-mean Gaussian vector $\boldsymbol{\eta}$ can be obtained from the expansion

$$\eta_i = \sum_{q=1}^{M} \sqrt{\lambda_q} z_{iq} \varphi_q \tag{5}$$

where λ_q and z_{iq} are respectively the q-th eigenvalue and the (i, q) component of the matrix of eigenvectors of the covariance matrix Σ, $\boldsymbol{\varphi} = (\varphi_1, \ldots, \varphi_M)$ are standard Gaussian random variables quantifying the uncertainty in geometry, and M denotes the number of most important terms in the expansion retained that correspond to the highest eigenvalues of the covariance matrix. Using the linear relationship [25] between the spatial distribution of the points along the airfoil profile and the Bézier control points, the properties of the Gaussian random field characterizing the spatial distribution of the variability in the airfoil profile can be readily obtained.

In this study, without loss of generality for the theory presented, the Euler equations for the 2-D compressible inviscid flows are solved and flow-related uncertainties as well as airfoil geometrical uncertainties are considered. Thus the vector of uncertain parameters $\mathbf{v} = (\boldsymbol{\theta}, \boldsymbol{\varphi})$ includes the uncertain flow conditions $\boldsymbol{\theta}$ (Mach number and angle of attack) and the vector of variables $\boldsymbol{\varphi}$, that corresponds to the geometrical uncertainties. Without loss of generality, a Gaussian distribution is also assumed for the flow conditions. Although in this study the uncertain parameters are assumed to follow a Gaussian distribution, different distributions may be also accounted using the appropriate quadrature rule. Also,

a histogram (which amounts to a PDF) can be constructed, based on actual flight conditions [24].

2.3. Formulation of shape optimization under uncertainties

The output flow quantities such as drag coefficient $C_D(\boldsymbol{\rho}, \mathbf{v})$ and lift coefficient $C_L(\boldsymbol{\rho}, \mathbf{v})$ given the values of the design variables $\boldsymbol{\rho}$ are uncertain due to the uncertainty in the parameters $\mathbf{v}$. The optimal aerodynamic shape of an airfoil under uncertainties should be selected to minimize a robust measure of the drag coefficient that takes into account the uncertainties in the model parameters and at the same time to be insensitive to uncertainties. For this, the robust aerodynamic optimization is formulated as a two-objective optimization problem with the objectives being the expected value $\mu_{C_D}(\boldsymbol{\rho})$ and standard deviation $\sigma_{C_D}(\boldsymbol{\rho})$ of the drag coefficient $C_D(\boldsymbol{\rho}, \mathbf{v})$ with respect to uncertainties $\mathbf{v} = (\boldsymbol{\theta}, \boldsymbol{\varphi})$ in flow conditions ($\boldsymbol{\theta}$) and geometrical control points ($\boldsymbol{\varphi}$). The mean is used as a robust measure of the drag coefficient that takes into account the uncertainties in the model parameters. The standard deviation is used as a measure of the sensitivity of the drag coefficient to uncertainties in the model parameters, providing optimal shapes that are robust to variabilities in the model parameters.

The optimal shape of the airfoil should also satisfy the lift constraint for all possible values of the model parameters. The implementation of this condition is not practical for most problems and may lead to substantial performance deterioration due to considerable increase of the drag arising from parameter values with low plausibility. Alternatively, the lift constraint can be imposed in a probabilistic manner, requiring that the probability the lift falls below a reference lift value is less than an acceptably small predefined probability. The optimal shape is then controlled by the user-assigned probability level of unacceptable performance for the lift.

Thus, in this study, the aerodynamic shape optimization of an airfoil under uncertainties in the flow conditions and geometrical parameters is mathematically formulated as

$$\min_{\boldsymbol{\rho}} \quad G_{C_D}(\boldsymbol{\rho}) = w\mu_{C_D}(\boldsymbol{\rho}) + (1-w)\sigma_{C_D}(\boldsymbol{\rho}) \tag{6a}$$

$$s.t. \quad Pr(C_L(\boldsymbol{\rho}, \mathbf{v}) \le C_{L,ref}) < P_{f,0} \tag{6b}$$

where the two measures for the mean and the standard deviation of the drag coefficient are concatenated to a single objective by introducing the weight w, and $Pr(C_L(\boldsymbol{\rho}, \mathbf{v}) \le C_{L,ref})$ is the probability of failure or probability of unacceptable performance, i.e. the probability the lift coefficient function C_L is lower than the reference value $C_{L,ref}$. The minimization for different values of w results in different optimal designs that form a Pareto front [27,39].

The constrained optimization problem is solved using a gradient-based method, requiring the derivatives of the output flow quantities with respect to design variables and uncertain parameters. The methodology for the computation of the function $G_{C_D}(\boldsymbol{\rho})$ and its derivatives with respect to the shape controlling design parameters $\boldsymbol{\rho}$ is exposed in Section 3.1. The estimation of the probability $P(C_L(\boldsymbol{\rho}, \mathbf{v}) \le C_{L,ref})$ and its derivatives with respect to the design parameters is described in Section 3.2. The derivatives of $G_{C_D}(\boldsymbol{\rho})$ and $P(C_L(\boldsymbol{\rho}, \mathbf{v}) \le C_{L,ref})$ with respect to the design variables $\boldsymbol{\rho}$ require the sensitivities of the drag and lift coefficient functions with respect to the design and uncertain parameters. The adjoint approach to compute such sensitivities is presented in Section 4.

3. Robust performance and reliability constraint

3.1. Robust drag

The mean and standard deviation of the objective function in (6a) are given in terms of the first two statistical moments $\bar{\mu}_{\gamma,C_D}(\boldsymbol{\rho})$, $\gamma = 1, 2$ of the multidimensional performance function $C_D(\boldsymbol{\rho}, \mathbf{v})$ as

$$\mu_{C_D}(\boldsymbol{\rho}) = \bar{\mu}_{1,C_D}(\boldsymbol{\rho}) \qquad \text{and} \qquad \sigma_{C_D}(\boldsymbol{\rho}) = \sqrt{\bar{\mu}_{2,C_D}(\boldsymbol{\rho}) - \mu^2_{C_D}(\boldsymbol{\rho})} \tag{7}$$

where

$$\bar{\mu}_{\gamma,C_D}(\boldsymbol{\rho}) = \int_V [C_D(\boldsymbol{\rho}, \mathbf{v})]^\gamma \, p(\mathbf{v}) d\mathbf{v} \tag{8}$$

The robust shape optimization requires the computation of the multi-dimensional integrals (8) for $\gamma = 1, 2$. Assuming that the PDF $p(\mathbf{v})$ of the uncertain parameters is Gaussian, the Gauss–Hermite quadrature on sparse grids [47,5,14] is used to approximate the integrals in the form [14]

$$\int_V [C_D(\boldsymbol{\rho}, \mathbf{v})]^\gamma \, p(\mathbf{v}) d\mathbf{v} \simeq \sum_{k=1}^{n} w_k {C_D}^\gamma(\boldsymbol{\rho}, \mathbf{v}_k) = \sum_{k=1}^{n} w_k C^\gamma_{D_k}(\boldsymbol{\rho}) \tag{9}$$

where $\mathbf{v}_k$ are the locations of the grid points in the uncertain parameter space and w_k are weighting coefficients, both depending on the order of the sparse grid formulation. $\mathbf{C_D} = (C_{D1}, \ldots C_{Dn})$ and $C_{D_k}(\boldsymbol{\rho}) \equiv C_D(\boldsymbol{\rho}, \mathbf{v}_k)$ is the value of the function C_D evaluated at the design variable value $\boldsymbol{\rho}$ and the value $\mathbf{v}_k$ of the uncertain parameter vector at the grid or sample points $\mathbf{v}_k$, $k = 1, \ldots, n$ in the uncertain parameter space. Alternatively, using MC methods, the sample estimates of the multidimensional integrals for the first two moments are given by (9), where $\mathbf{v}_k$ are the samples generated from the PDF $p(\mathbf{v})$.

The robust objective function $G_{C_D}(\boldsymbol{\rho})$ is thus given as a function of the performance values $C_{D1}, \ldots, C_{Dn}$ evaluated at the sparse grid or sample points, as follows

$$G_{C_D}(\boldsymbol{\rho}) = w\,\mu_{1,C_D}(\boldsymbol{\rho}) + (1-w)\sqrt{\mu_{2,C_D}(\boldsymbol{\rho}) - \mu^2_{1,C_D}(\boldsymbol{\rho})} \tag{10}$$

The first order sensitivities of $G_{C_D}(\boldsymbol{\rho})$ with respect to the design parameters $\boldsymbol{\rho} = (\rho_1, \ldots, \rho_N)^T$, where N is the number of design variables, required in the gradient-based optimization algorithm, are given by

$$\frac{\partial G_{C_D}(\boldsymbol{\rho})}{\partial \rho_i} = \sum_{k=1}^{n} \frac{\partial G_{C_D}}{\partial C_{Dk}} \frac{\partial C_{Dk}}{\partial \rho_i} = \sum_{k=1}^{n} a_k \frac{\partial C_D(\boldsymbol{\rho}, \mathbf{v}_k)}{\partial \rho_i} \tag{11}$$

where the coefficients a_k, given by

$$a_k = \frac{\partial G(\mathbf{C_D})}{\partial C_{Dk}} = w w_k + (1-w) w_k \frac{C_{Dk} - \mu_{1,C_D}(\mathbf{C_D})}{\sigma_{C_D}(\mathbf{C_D})} \tag{12}$$

depend on the value of the performance function $C_{Dk} = C_D(\boldsymbol{\rho}, \mathbf{v}_k)$ at the grid points $k = 1, \ldots, n$. The sensitivities of $G_{C_D}(\boldsymbol{\rho})$ with respect to the design variables $\boldsymbol{\rho}$ depend on the sensitivities of the performance function $C_D(\boldsymbol{\rho}, \mathbf{v})$ in (11) with respect to the design variables $\boldsymbol{\rho}$, evaluated at the grid or sample points $\mathbf{v}_k$. These sensitivities are computed using the adjoint formulation for the flow as described in Section 4.

3.2. Lift reliability

The probability the lift coefficient $C_L(\boldsymbol{\rho}, \mathbf{v})$ is lower than a predefined reference value $C_{L,ref}$ is given by

$$P_f(\boldsymbol{\rho}) \equiv Pr(C_L(\boldsymbol{\rho}, \mathbf{v}) < C_{L,ref}) = Pr(h(\boldsymbol{\rho}, \mathbf{v}) < 0) = \int_{h(\boldsymbol{\rho}, \mathbf{v}) < \mathbf{0}} p(\mathbf{v}) \mathbf{dv} \tag{13}$$

where $h(\boldsymbol{\rho},\mathbf{v}) = C_L(\boldsymbol{\rho},\mathbf{v}) - C_{L,ref}$ is the limit state function in reliability terminology [10]. Using FORM, $P_f(\boldsymbol{\rho})$ is approximated by the expression [10]

$$P_f(\boldsymbol{\rho}) \approx \Phi(-\beta(\boldsymbol{\rho})) \tag{14}$$

where Φ is the standard normal cumulative distribution function and $\beta(\boldsymbol{\rho})$ is computed by the expression [9,13,1]

$$\beta(\boldsymbol{\rho}) = -\frac{\mathbf{v}^T \nabla_{\mathbf{v}} C_L|_{\mathbf{v}=\mathbf{v}^*}}{\|\nabla_{\mathbf{v}} C_L\|_{\mathbf{v}=\mathbf{v}^*}} \tag{15}$$

where $\mathbf{v}^* = \mathbf{v}^*(\boldsymbol{\rho})$ is the design point that is computed for given $\boldsymbol{\rho}$ by solving the following optimization sub-problem in the uncertain space $\mathbf{v} = (v_1, \ldots, v_n)$ of the standard Gaussian normal variables

$$\min_{\mathbf{v}} \quad \|\mathbf{v}\|^2 = \mathbf{v}^T\mathbf{v} \tag{16a}$$

$$s.t. \quad C_L(\boldsymbol{\rho},\mathbf{v}) - C_{L,ref} = 0 \tag{16b}$$

and $\|\cdot\|$ denotes the Euclidean norm. The computation of failure probability and the search for the design point $\mathbf{v}^*(\boldsymbol{\rho})$ in the uncertain parameter space using gradient-based optimization techniques requires the sensitivities of the lift coefficient function $C_L(\boldsymbol{\rho},\mathbf{v})$ with respect to the uncertain parameters, i.e. $\frac{\partial C_L}{\partial v_k}$. Using the expansion (5), the sensitivity of the lift coefficient with respect to the uncertain parameters φ_k in $\mathbf{v} = (\boldsymbol{\theta},\boldsymbol{\varphi})$ are given by

$$\frac{\partial C_L}{\partial \varphi_k} = \sum_{i=1}^{N} \frac{\partial C_L}{\partial \rho_i} \sqrt{\lambda_k} z_{ik} \tag{17}$$

The sensitivities of the probability of unacceptable performance with respect to the design variables, required to drive a descent optimization algorithm, are computed by [13,9,1]

$$\frac{\partial P_f(\mathbf{C_L})}{\partial \rho_i} = \frac{\partial \Phi(-\beta(\boldsymbol{\rho}))}{\partial \rho_i} = \gamma(\boldsymbol{\rho},\mathbf{v}^*)\frac{\partial C_L}{\partial \rho_i} \tag{18}$$

where $\gamma(\boldsymbol{\rho},\mathbf{v}^*)$ is given by

$$\gamma(\boldsymbol{\rho},\mathbf{v}^*) = -\frac{exp\left(-\beta^2(\boldsymbol{\rho})/2\right)}{\sqrt{2\pi}\|\nabla_{\mathbf{v}} C_L\|_{\mathbf{v}=\mathbf{v}^*}} \tag{19}$$

The estimation of $\frac{\partial P_f(\mathbf{C_L})}{\partial \boldsymbol{\rho}}$ depends on the sensitivities $\frac{\partial C_L}{\partial v_k}$ of the lift coefficient C_L with respect to the uncertain parameters v_k, evaluated at the design point $\mathbf{v}^*$ in the uncertain parameter space and the sensitivities $\frac{\partial C_L}{\partial \boldsymbol{\rho}_i}$ of the lift coefficient with respect to the design variables $\boldsymbol{\rho}$. Both types of sensitivities are computed using the adjoint formulation as described in Section 4.

4. The adjoint method for the computation of flow sensitivities

4.1. Flow equations

The governing flow (state) equations are the Euler equations for 2D compressible flows. The Euler equations for a compressible inviscid flow are cast in tensor form as

$$\frac{\partial U_n}{\partial t} + \frac{\partial f_{nk}}{\partial x_k} = 0 \tag{20}$$

where the Einstein notation is assumed for repeated indices and t is the pseudo-time. The conservative variables U_n and the fluxes f_{nk} are given by

$$U = \begin{bmatrix} U_1 \\ U_2 \\ U_3 \\ U_4 \end{bmatrix} = \begin{bmatrix} \rho \\ \rho u_1 \\ \rho u_2 \\ E \end{bmatrix}, \quad \begin{bmatrix} f_{1k} \\ f_{2k} \\ f_{3k} \\ f_{4k} \end{bmatrix} = \begin{bmatrix} \rho u_k \\ \rho u_1 u_k + p\delta_{k1} \\ \rho u_2 u_k + p\delta_{k2} \\ u_k(E+p) \end{bmatrix} \tag{21}$$

In Eq. (21), ρ, u_k and $E = \rho e + \frac{1}{2}\rho u_k^2$ stand for the density, the velocity components and total energy per unit volume, respectively. Also, δ_{km} is the Kronecker symbol.

A vertex-centered finite volume method is used for the discretization of Eq. (20). Inviscid fluxes crossing the control volume boundaries are computed using the Roe's upwind scheme [44].

4.2. The adjoint formulation

The sensitivity derivatives of the objective and constraint functions are computed using the discrete adjoint approach. The derivatives of the function F ($F \equiv C_D$ or $F \equiv C_L$) with respect to the control variables $\mathbf{b}$, which can be either the design variables ($\mathbf{b} \equiv \boldsymbol{\rho}$) or the uncertain parameters ($\mathbf{b} \equiv \mathbf{v}$), are computed as follows. F depends on $\mathbf{b}$ directly and indirectly through the state variables $\mathbf{U}$, i.e. $F = F(\mathbf{U}(\mathbf{b}),\mathbf{b})$. $\mathbf{U}$ satisfy the state equations $\mathbf{R}(\mathbf{U}(\mathbf{b}),\mathbf{b}) = \mathbf{0}$, which are formed by the discretization of Eq. (20).

The sensitivity derivatives of F with respect to b_i are computed using the chain rule

$$\frac{dF}{db_i} = \frac{\partial F}{\partial b_i} + \frac{\partial F}{\partial U_k}\frac{dU_k}{db_i} \tag{22}$$

where the sensitivity fields $\frac{dU_k}{db_i}$ are computed by solving the equations

$$\frac{dR_m}{db_i} = \frac{\partial R_m}{\partial b_i} + \frac{\partial R_m}{\partial U_k}\frac{dU_k}{db_i} = 0 \tag{23}$$

Eqs. (22) and (23) constitute the so-called direct differentiation or forward approach and its cost scales with the number of control variables. Alternatively, one may refer to the adjoint approach. In that case the derivatives $\frac{dF}{db_i}$ are computed by the expression [38,4,31]

$$\frac{dF}{db_i} = \frac{\partial F}{\partial b_i} + \Psi_m \frac{\partial R_m}{\partial b_i} \tag{24}$$

where the so-called adjoint variables Ψ_m are computed by solving the adjoint equations, expressed as [38,4,31]

$$\frac{\partial F}{\partial U_k} + \Psi_m \frac{\partial R_m}{\partial U_k} = 0 \tag{25}$$

The cost of the adjoint approach is independent of the number of design variables, being almost equal to that of solving the state equations.

It should also pointed out that the partial or direct sensitivities $\frac{\partial F}{\partial b_i}$, $\frac{\partial F}{\partial U_k}$, $\frac{\partial R_m}{\partial b_i}$ and $\frac{\partial R_m}{\partial U_k}$ of the objective function F and the residuals of the flow equations R_m with respect to the control parameters b_i and the flow variables U_k, which are required in both the direct differentiation and the adjoint approach are computed using analytical expressions with a cost lower than that of solving the flow, adjoint and direct differentiation equations. However, for cases where analytical expressions are not available, the cost of computing some of the partial terms with finite differences may be significant, especially for 3D cases with large number of grid points and design variables. The cost for the computation of the sensitivities, Eqs. (22) and (24), is also negligible compared to the cost of solving the direct differentiation or the adjoint equations, i.e. equations (23) or (25). Also, since the cost for solving equations (23) scales with the number of design variables in contrast to equations (25), which have to be solved only once, irrespective of the number of design variables, it is obvious that the adjoint approach outperforms the direct differentiation one.

Using the adjoint approach the sensitivities of the objective function with respect to the shape controlling parameters and the uncertain parameters are computed at a cost independent of the number of these parameters.

Algorithm 1: Pseudo-code for shape optimization under uncertainties.

```
% Iterative estimation of optimal values of design variables ρ
k ← 0
ρ_k ← Init()
while k ≤ k_max, (Outer Loop Optimization) do
  % Estimate robust performance and sensitivities to design variables
  for i ≤ n, (Sparse Grid Points) do
    θ(i), φ(i) ← Sparse Grid Gauss Hermite Quadrature
    η(i), ρ̃(i) ← Expansion (5) and Eq. (4)
    U(i) ← Solve Flow Equations, Eq. (20)
    C_D(i) ← Estimation of Drag Coefficient, Eq. (2)
    Ψ(i) ← Solve Adjoint Equations, Eq. (25)
    ∂C_D/∂b (i) ← Estimation of Drag Coefficient Sensitivities, Eq. (24)
  end for
  G ← Robust Performance, Eqs. (10) and (9)
  ∂G(C_D)/∂ρ ← Robust Performance Sensitivities, Eqs. (11) and (12)
  % Estimate probability of failure and sensitivities to design variables and uncertain parameters
  θ, φ ← Init()
  while m ≤ m_max, (Inner Loop for Reliability Design Point given ρ_k) do
    U ← Solve Flow Equations, Eq. (20)
    L ← Estimation of Lift Coefficient, Eq. (2)
    Ψ ← Solve Adjoint Equations, Eq. (25)
    ∂C_L/∂θ (i) ← Lift Coefficient Sensitivities wrt Flow, Eq. (24)
    ∂C_L/∂φ (i) ← Lift Coefficient Sensitivities wrt Geometry, Eq. (24)
    dθ, dφ ← Optimization Algorithm
    (θ, φ) ← (θ, φ) + d(θ, φ)
  end while
  θ*, φ* ← θ, φ
  P_f ← Probability of Failure, Eq. (14)
  ∂P_f(C_L)/∂ρ ← Probability of Failure Sensitivities, Eq. (18)
  % Update design variables
  ρ_k ← ρ_k + dρ
  k ← k + 1
end while
```

5. Pseudo-algorithm for shape optimization under uncertainties

The pseudo-code for the robust drag coefficient minimization with lift coefficient reliability constraint is summarized in Algorithm 1.

At each iteration of the outer loop, the optimizer requires n solutions of the flow and adjoint equations at the sparse grid points for computing the robust performance and its sensitivity with respect to the design variables, as well as M solutions of the flow and adjoint equations at the M iteration points involved in the inner loop for computing the probability of failure and its sensitivity with respect to the design variables and uncertain parameters. The n solutions of the flow and adjoint equations at the sparse grid or sample points are independent and can be performed in parallel. Thus, the time-to-solution in a parallel implementation of the algorithm is the time required to solve M flow and adjoint equations. To keep M small, the starting point of the inner optimization loop for the current iteration is selected to be the optimal point found in the previous iteration. This is expected to accelerate convergence to the design point with the fewer possible iterations. The total time-to-solution in a parallel implementation is independent of the number of sparse grid points.

6. Application

The proposed methodology is applied to the robust aerodynamic shape optimization with reliability constraint of an airfoil under uncertainties in the flow conditions and geometrical parameters. The symmetric RAE 2822 airfoil, which is a widely optimized configuration in the literature [45,6] is considered as the initial configuration and 13 Bézier control points are used to parameterize each airfoil side. The first and last control points are kept constant and the remaining ones are allowed to vary at the direction normal to the chord constrained within a box of dimension 0.01. The mean value of the angle of attack is also considered as a design variable. Thus, the total number of design parameters is equal to $11+11+1=23$. The initial parameterization of the airfoil with the Bézier points is plotted in Fig. 1.

The flow related uncertain parameters consist of the Mach number and the angle of attack, each one considered to follow a Gaussian distribution. The mean value of the Mach number is equal to $\mu_M = 0.73$. Its standard deviation is considered equal to $\sigma_M = 0.03$ corresponding to a coefficient of variation (COV) equal to 4.11%. The mean value of the angle of attack is equal to $\mu_\alpha = 2^\circ$ with a standard deviation equal to $\sigma_\alpha = 0.2^\circ$, corresponding to a COV equal to 10%. The mean values and standard deviations are similar to those considered in the literature [45].

The geometrical uncertainties are taken into account by applying the expansion (5) for the design parameters that separately define the pressure side and the suction side of the airfoil. Using a covariance function $\Sigma_{ij} = \sigma^2 exp\left(-\frac{r_{ij}}{\lambda}\right)$ with $\lambda = 0.3$ it can be demonstrated that only the first four terms in the expansion (5) contribute to the uncertainty. Retaining only the four highest

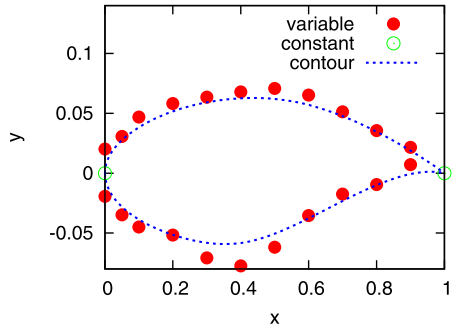

Fig. 1. Initial set of 13 per side Bézier control points parameterizing the RAE 2822 airfoil. The first and last of them per side are kept constant and the normal to the chord coordinates of the remaining $11+11=22$ control points constitute the geometrical design parameters of the problem.

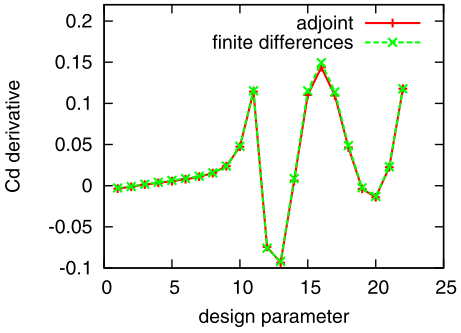

Fig. 2. Derivatives of the drag coefficient with respect to the geometrical design parameters for the initial airfoil, using the adjoint approach and finite differences.

eigenvalues for each airfoil side ($M=4$) results in a total number of uncertain parameters equal to 10. The standard deviation σ in the geometric parameters is chosen to be $\sigma=0.0004$ so as to allow the shape to vary by 1% which is a reasonable value that could arise from manufacturing imprecisions.

The constraint for the lift coefficient is set in this case to $C_{L,ref}=0.3$ and the bound for probability of unacceptable performance is set to $P_{f,0}=0.01$. Other values for this probability are also considered to scrutinize their effect in the optimal shape. A first-order sparse grid has been used to estimate the integrals based on Eq. (9), requiring 21 sparse grid points. Higher-order sparse grids made no difference in the mean value of the performance function (less than 1% difference) and a small difference in its standard deviation (about 10% difference). Also, the weight function w in the robust objective (6a) is chosen to be equal to 0.5.

The Euler equations are solved for the transonic flow problem aiming mostly to illustrate the performance of the algorithm. The formulation can be extended for other flow cases such as a fully turbulent flow, by implementing an appropriate turbulence model.

6.1. Deterministic optimization

The sensitivity derivatives of the drag coefficient and the lift coefficient with respect to the 22 geometrical parameters are shown in Figs. 2 and 3, respectively, for the initial values of the design variables and the mean values of the uncertain parameters. The comparison between the implemented adjoint approach and the finite differences is satisfactory. The finite differences were computed using a step size equal to 10^{-7}. A step size study was conducted which resulted to almost exactly the same finite differences for different orders of magnitude of the step size value. The L2 norm of the error is equal to 0.16% for the drag and 6.3% for the lift coefficient. For most design parameters adjoint and finite difference sensitivity values agree up to 2 to 3 digits.

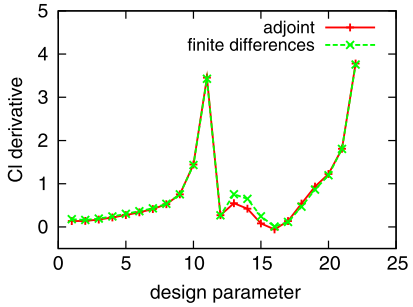

Fig. 3. Derivatives of the lift coefficient with respect to the geometrical design parameters for the initial airfoil, using the adjoint approach and finite differences.

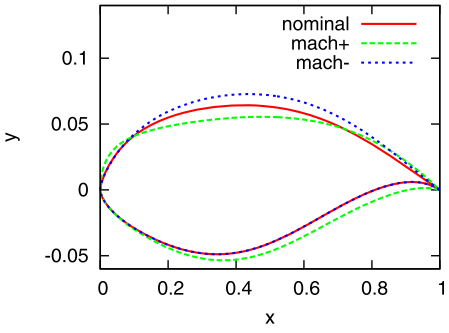

Fig. 4. Optimal airfoil shape obtained by deterministic optimization, i.e. minimization of drag coefficient constrained by minimum allowed lift coefficient, for different values of the Mach uncertain parameter corresponding to the first level grid points.

The deterministic optimization with deterministic constraint for different values of the Mach uncertain parameter has also been conducted to make some first observations for the different optimal shapes. The values of the other uncertain parameters are kept constant at their mean values. The optimal airfoil shapes that correspond to the solutions of the three deterministic optimization problems are plotted in Fig. 4.

6.2. Optimization under uncertainties

The optimization is based on the minimization of the weighted sum of the mean value and standard deviation of the drag coefficient subject to the probability of the lift coefficient to exceed a reference value $C_{L,ref}$ is less that a predefined probability $P_{f,0}$. $C_{L,ref}$ is set to 0.3. Parametric studies with respect to the value of this predefined probability $P_{f,0}$, as well as the standard deviations of the uncertain parameters are conducted. The mean value and standard deviation of the objective function are computed using the sparse grid approach in terms of the drag coefficient performance values at the nodes of the sparse grid. The constraint value is computed using the reliability-based analysis, based on the FORM approach.

The derivatives of the mean value and standard deviation of the drag coefficient with respect to the design parameters are plotted in Fig. 5 for the initial airfoil shape. The derivatives of the probability the lift coefficient exceeds the reference lift coefficient value, with respect to the design parameters are plotted in Fig. 6 for the initial airfoil shape.

Four different design cases are first compared:

1. Deterministic drag coefficient performance with deterministic lift coefficient constraint (DeDe): The objective function is the drag coefficient computed for the mean values of the flow conditions and with no geometric uncertainties. The inequality constraint function is the difference of the lift coefficient com-

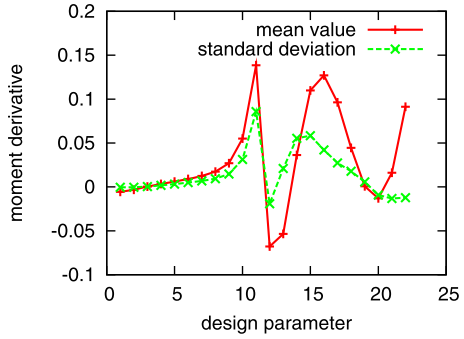

Fig. 5. Derivatives of the mean value and standard deviation of the drag coefficient for the initial airfoil with respect to the geometrical design parameters.

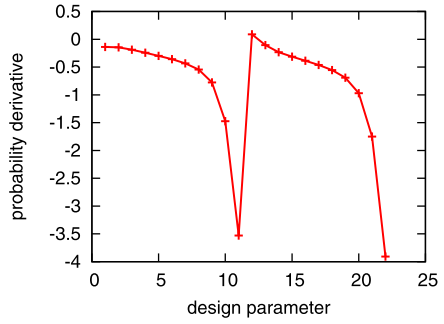

Fig. 6. Derivatives of the probability of the lift to be less than a reference lift value, for the initial airfoil with respect to the geometrical design parameters.

puted for the mean values of the uncertain parameters from the lift coefficient reference value $C_{L,ref}$.

2. Robust drag coefficient performance with deterministic lift coefficient constraint (RoDe): The objective is the weighted sum of the mean value and standard deviation of the drag coefficient computed through the sparse grid quadrature. The inequality constraint is the same as in the DeDe design case.
3. Deterministic drag coefficient performance with lift coefficient reliability constraint (DeRe): The objective is the same as in the DeDe design case. The inequality constraint is the difference of the probability the lift coefficient to be less than a lift coefficient reference value $C_{L,ref}$ from a predefined probability value $P_{f,0}$.
4. Robust drag coefficient performance with lift coefficient reliability constraint (RoRe): The objective is same as in the RoDe robust design case and the constraint is the same as in the DeRe reliability constraint design case.

Comparisons are made in terms of:

- The drag coefficient $C_D(\mu_c)$ for the mean values of the uncertain parameters,
- the mean value μ_{C_D} of the drag coefficient,
- the standard deviation σ_{C_D} of the drag coefficient and
- the probability of the lift to be less than the reference lift value $C_{L,ref}$.

The comparison is summarized in Table 1 and the optimal airfoils are shown in Fig. 7. As expected, the lower value for $C_D(\mu_c)$ is obtained in the DeDe design case where uncertainties are ignored. The large $\sigma_{C_D} = 0.001579$ value obtained in relation to the design cases RoDe and RoRe indicates that the DeDe design case is very sensitive to uncertainties for the specific mean values and standard deviations considered for the Mach value and angle of attack. The value of $\sigma_{C_D} = 0.000044$ is one order less than the DeDe design case, indicating that the RoDe design case is significantly less sensitive to uncertainties. In the DeRe design case of lift coefficient reliability constraint, the probability of unacceptable performance for the lift coefficient attains its bound $P_{f,0}$ but, due to higher values for μ_{C_D} and σ_{C_D} than the RoDe and DeDe cases, the optimal design is substantially less robust, with the drag coefficient to be most sensitive to variations in the uncertain parameters. In the RoRe design case of robust drag and lift coefficient reliability constraint, the lift coefficient constraints are satisfied with the bound probability $P_{f,0}$ as in the DeRe design case, but with mean μ_{C_D} and the standard deviation σ_{C_D} values of the drag coefficient that are smaller than the optimal designs in the DeDe and the DeRe cases. The RoRe design case corresponds to drag coefficient values that are most robust to uncertainties, satisfying the reliability constraints for the lift.

Table 1
Comparison of the objective function value, mean value, standard deviation and probability of failure for the DeDe, RoDe, DeRe and RoDe designs.

Design cases	$C_D(\mu_c)$	μ_{C_D}	σ_{C_D}	P_f
DeDe	0.00219	0.00422	0.00457	0.50
RoDe	0.00274	0.00318	0.00124	0.48
DeRe	0.00305	0.00550	0.00572	0.01
RoRe	0.00378	0.00479	0.00256	0.01

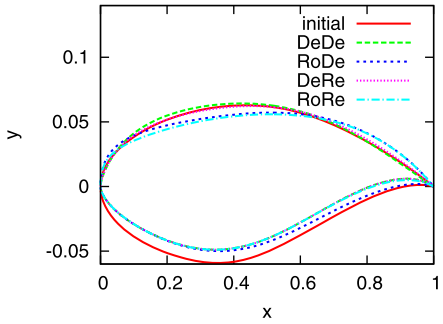

Fig. 7. Optimal airfoil shape obtained by DeDe, RoDe, DeRe and RoRe design cases.

Fig. 7 indicates that the optimal shapes depend on the design cases considered. Uncertainties in the drag and lift coefficients affect the resulting optimal shapes. Thus, it is important for the designer to be aware of the uncertainties of the parameters as well as the objectives and constraints that really matter for the design. The convergence rates of the mean value, standard deviation and probability of failure constraint for the RoRe case are shown in Fig. 8. Full convergence is obtained within about 100 optimization cycles. Similar rates have been observed for the rest of the cases.

The optimal shapes for the RoRe design case and for different values of the probabilistic constraint ($P_{f,0} = 0.1, 0.01, 0.005$) are plotted in Fig. 9 while in Table 2, the optimal values for the drag coefficient nominal value, mean value and standard deviation are shown. It can be seen that only the pressure side contours of the optimal airfoil shapes depend on the reliability level $P_{f,0}$. Also, there is a trade-off between mean drag reduction μ_{C_D}, along with the drag sensitivity to uncertainty σ_{C_D}, and the probability of failure for the lift condition. Imposing strict conditions on the lift coefficient constraint to be satisfied with very high reliability or very small probability of unacceptable performance, considerably affects the drag coefficient by increasing its mean value and its sensitivity to uncertainty.

The individual contribution of the two types of uncertainties, i.e. the uncertainties in the flow conditions and the geometrical uncertainties is also investigated for the RoRe design case. The optimal airfoil shape obtained by considering uncertainties (a) only in the Mach number and the angle of attack and (b) in Mach number, angle of attack and geometrical parameters, are compared

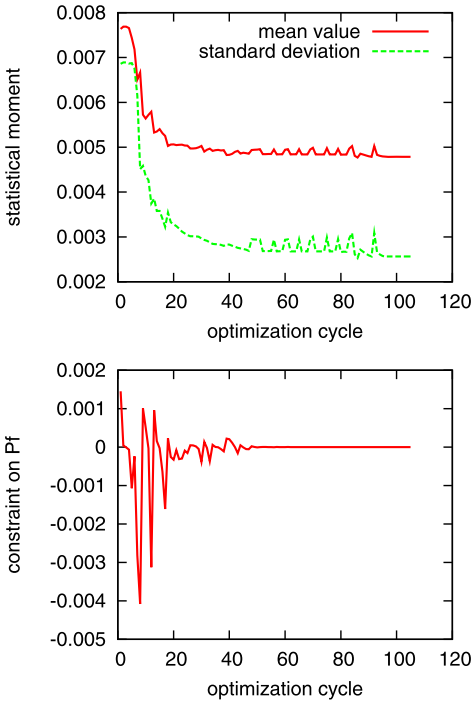

Fig. 8. Convergence rates of mean value, standard deviation and probability of failure constraint for the RoRe case.

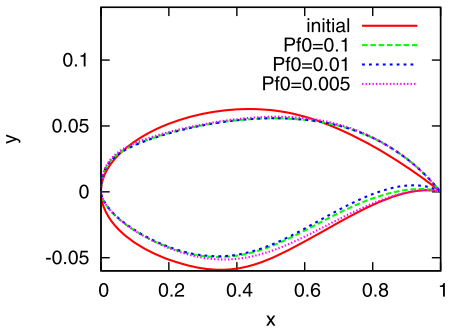

Fig. 9. Optimal airfoil shape obtained by the RoRe design case for different values of the probability $P_{f,0}$ for $w = 0.5$.

Table 2
Comparison of the nominal value, mean value and standard deviation of the drag coefficient for different values of the probability of failure in the RoRe design case.

	$C_D(\mu_c)$	μ_{C_D}	σ_{C_D}	P_f
$P_{f_0} = 0.005$	0.00457	0.00577	0.00312	0.005
$P_{f_0} = 0.01$	0.00378	0.00479	0.00256	0.01
$P_{f_0} = 0.1$	0.00331	0.00408	0.00191	0.1

with each other in Fig. 10 and the corresponding values of mean value and standard deviation of the drag coefficient and probability of failure for the lift are included in Table 3. It can be deduced that the inclusion of only flow related uncertainties has the major effect on the optimal airfoil shape. The inclusion of the geometrical uncertainties slightly affects, in this case, the trailing edge of the airfoil.

7. Conclusions

A framework for aerodynamic shape optimization under uncertainty was presented. The optimal design minimizes a measure of the drag coefficient that is robust to uncertainties, subject to the lift coefficient reliability constraint. The multi-dimensional integrals for the mean and standard deviation of the drag coefficient were computed by the sparse grid technique, while the reliability was computed using FORM. The design parameters were the coordinates of the Bézier control points parameterizing the airfoil shape. The uncertain parameters were the flow conditions (Mach number and angle of attack) and the coordinates of the Bézier control points (design variables), accounting through the airfoil contour parameterization for the geometric variabilities of the airfoil. The sensitivities of the robust measure of the drag coefficient and the lift reliability constraint with respect to the design variables and uncertain parameters were computed by the discrete adjoint approach to the Euler equations, substantially reducing the number of flow solutions to the solution on the forward and the adjoint equations, thus making the computational effort independent of the number of design variables and uncertain parameters. In parallel implementation of the proposed optimal shape optimization algorithm, the time-to-solution, which depends on the solution of the forward and adjoint flow equations, scales with the number of iterations required to estimate the FORM "design" point in the uncertain parameter space and it is independent of the number of sparse grid points.

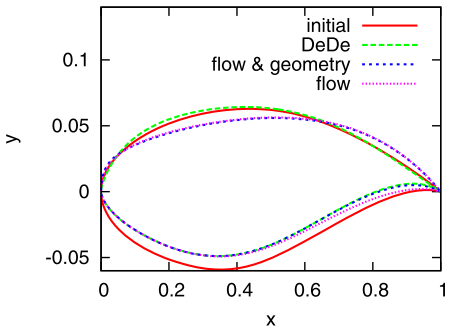

Fig. 10. Optimal airfoil shape obtained for the RoRe design cases for either flow-related uncertainties or both types of uncertainties.

Table 3
Comparison of the objective function value, mean value, standard deviation and probability of failure for the RoRe design cases taking into account either flow-related uncertainties only or both types of uncertainties.

	$C_D(\mu_c)$	μ_{C_D}	σ_{C_D}	P_f
flow	0.00369	0.00505	0.00333	0.01
flow & geometry	0.00378	0.00479	0.00256	0.01

Applications demonstrated that the proposed approach provides optimal airfoil shape that are least sensitive to uncertainties, meeting at the same time the pre-imposed lift reliability constraints. Parametric studies have shown the important influence of the magnitude of uncertainties and the probability of failure threshold values. Each type of uncertainty (flow-related and geometrical) affects differently the optimal airfoil shape and the performance. The studies demonstrate the importance of considering uncertainties in the design so that the optimal airfoil shape maintains its functionality over the whole range of variation of the uncertain model parameters. It provides a new perspective for meeting the lift coefficient constraints in a probabilistic manner, guarantying that the design goals are met within a user-defined probability. A trade-off between mean drag over the uncertain domain and drag sensitivity to uncertainties was demonstrated. A trade-off between robust drag and lift reliability was also observed. The smaller the probability of unacceptable performance, the less effective the performance on the robust drag coefficient, increasing the drag value in order to meet the lift probability constraints.

Finally, FORM techniques provide an approximation to the multi-dimensional lift reliability integral. In addition, implementation difficulties are also expected when multiple "design" points

are manifested that complicate the use of FORM due to difficulties in identifying the number and location of the multiple "design" points in the uncertain parameter space. These deficiencies in FORM can be overcome and considerably improve accuracy by employing advanced sampling techniques [49,29,18,3] to estimate the lift reliability integrals in the expense of higher computational effort, but the implementation of these techniques is beyond the scope of this paper.

Conflict of interest statement

There is no conflict of interest.

Acknowledgements

The research project is implemented within the framework of the Action "Supporting Postdoctoral Researchers" of the Operational Program "Education and Lifelong Learning" (Action's Beneficiary: General Secretariat for Research and Technology), and is co-financed by the European Social Fund (ESF) and the Greek State.

References

[1] M. Allen, K. Maute, Reliability-based design optimization of aeroelastic structures, Struct. Multidiscip. Optim. 27 (4) (2004) 228–242.
[2] P. Angelikopoulos, C. Papadimitriou, P. Koumoutsakos, Bayesian uncertainty quantification and propagation in molecular dynamics simulations: a high performance computing framework, J. Chem. Phys. 137 (14) (2012) 144103.
[3] S.K. Au, Probabilistic failure analysis by importance sampling Markov chain simulation, J. Eng. Mech. 130 (3) (2004) 303–311.
[4] J. Brezillon, N.R. Gauger, 2d and 3d aerodynamic shape optimisation using the adjoint approach, Aerosp. Sci. Technol. 8 (8) (2004) 715–727.
[5] H.J. Bungartz, M. Griebel, Sparse grids, Acta Numer. 13 (2004) 147–269.
[6] G. Carrier, D. Destarac, A. Dumont, M. Meheut, I.S.E. Din, J. Peter, S.B. Khelil, J. Brezillon, M. Pestana, Gradient-based aerodynamic optimization with the elsA software, in: 52nd Aerospace Sciences Meeting, vol. 10, 2014, Conference Paper AIAA 2014-0568.
[7] S.H. Cheung, T.A. Oliver, E.E. Prudencio, S. Prudhomme, R.D. Moser, Bayesian uncertainty analysis with applications to turbulence modeling, Reliab. Eng. Syst. Saf. 96 (9) (2011) 1137–1149.
[8] P.J. Davis, P. Rabinowitz, Methods of Numerical Integration, Courier Corporation, 2007.
[9] A. Der Kiureghian, First- and second-order reliability methods, in: Engineering Design Reliability Handbook, 2005, chapter 14.
[10] O. Ditlevsen, H.O. Madsen, Structural Reliability Methods, vol. 178, Wiley, 1996.
[11] C. Dribusch, S. Missoum, P. Beran, A multifidelity approach for the construction of explicit decision boundaries: application to aeroelasticity, Struct. Multidiscip. Optim. 42 (5) (2010) 693–705.
[12] W.N. Edeling, P. Cinnella, R.P. Dwight, H. Bijl, Bayesian estimates of parameter variability in the k–ε turbulence model, J. Comput. Phys. 258 (2014) 73–94.
[13] I. Enevoldsen, J.D. Sørensen, Reliability-based optimization in structural engineering, Struct. Saf. 15 (3) (1994) 169–196.
[14] T. Gerstner, M. Griebel, Numerical integration using sparse grids, Numer. Algorithms 18 (3–4) (1998) 209–232.
[15] R.G. Ghanem, P.D. Spanos, Stochastic Finite Elements: A Spectral Approach, Courier Corporation, 2003.
[16] L. Huyse, S.L. Padula, R.M. Lewis, W. Li, Probabilistic approach to free-form airfoil shape optimization under uncertainty, AIAA J. 40 (9) (2002) 1764–1772.
[17] M. Jalalpour, J.K. Guest, T. Igusa, Reliability-based topology optimization of trusses with stochastic stiffness, Struct. Saf. 43 (2013) 41–49.
[18] H.A. Jensen, M.A. Valdebenito, G.I. Schueller, An efficient reliability-based optimization scheme for uncertain linear systems subject to general Gaussian excitation, Comput. Methods Appl. Mech. Eng. 198 (1) (2008) 72–87.
[19] H.A. Jensen, M.A. Valdebenito, G.I. Schueller, D.S. Kusanovic, Reliability-based optimization of stochastic systems using line search, Comput. Methods Appl. Mech. Eng. 198 (49) (2009) 3915–3924.
[20] H.S. Jung, S. Cho, Reliability-based topology optimization of geometrically nonlinear structures with loading and material uncertainties, Finite Elem. Anal. Des. 41 (3) (2004) 311–331.
[21] G. Kharmanda, N. Olhoff, A. Mohamed, M. Lemaire, Reliability-based topology optimization, Struct. Multidiscip. Optim. 26 (5) (2004) 295–307.
[22] S.T. LeDoux, J.C. Vassberg, D.P. Young, S. Fugal, D. Kamenetskiy, W.P. Huffman, R.G. Melvin, M.F. Smith, Study based on the AIAA aerodynamic design optimization discussion group test cases, AIAA J. 53 (7) (2015) 1910–1935.
[23] W. Li, L. Huyse, S. Padula, Robust airfoil optimization to achieve drag reduction over a range of Mach numbers, Struct. Multidiscip. Optim. 24 (1) (2002) 38–50.
[24] R.P. Liem, G.K.W. Kenway, J.R.R.A. Martins, Multimission aircraft fuel-burn minimization via multipoint aerostructural optimization, AIAA J. 53 (1) (2014) 104–122.
[25] G.G. Lorentz, Bernstein Polynomials, 2nd edition, Chelsea Publishing Co, New York, USA, 1986.
[26] Z. Lyu, G.K. Kenway, C. Paige, J.R.R.A. Martins, Automatic differentiation adjoint of the Reynolds-averaged Navier–Stokes equations with a turbulence model, in: 21st AIAA Computational Fluid Dynamics Conference, AIAA, Reston, VA, 2013, pp. 1–24.
[27] M. Martinelli, R. Duvigneau, On the use of second-order derivatives and metamodel-based Monte-Carlo for uncertainty estimation in aerodynamics, Comput. Fluids 39 (6) (2010) 953–964.
[28] K. Maute, D.M. Frangopol, Reliability-based design of MEMS mechanisms by topology optimization, Comput. Struct. 81 (8) (2003) 813–824.
[29] J.C. Medina, A. Taflanidis, Probabilistic measures for assessing appropriateness of robust design optimization solutions, Struct. Multidiscip. Optim. 51 (4) (2015) 813–834.
[30] K. Mogami, S. Nishiwaki, K. Izui, M. Yoshimura, N. Kogiso, Reliability-based structural optimization of frame structures for multiple failure criteria using topology optimization techniques, Struct. Multidiscip. Optim. 32 (4) (2006) 299–311.
[31] J.D. Müller, P. Cusdin, On the performance of discrete adjoint CFD codes using automatic differentiation, Int. J. Numer. Methods Fluids 47 (8–9) (2005) 939–945.
[32] M. Nikbay, M.N. Kuru, Reliability based multidisciplinary optimization of aeroelastic systems with structural and aerodynamic uncertainties, J. Aircr. 50 (3) (2013) 708–715.
[33] T.A. Oliver, R.D. Moser, Bayesian uncertainty quantification applied to RANS turbulence models, J. Phys. Conf. Ser. 318 (2011) 042032.
[34] S.L. Padula, C.R. Gumbert, W. Li, Aerospace applications of optimization under uncertainty, Optim. Eng. 7 (3) (2006) 317–328.
[35] M. Padulo, M.S. Campobasso, M.D. Guenov, Novel uncertainty propagation method for robust aerodynamic design, AIAA J. 49 (3) (2011) 530–543.
[36] C. Papadimitriou, J.L. Beck, L.S. Katafygiotis, Asymptotic expansions for reliability and moments of uncertain systems, J. Eng. Mech. 123 (12) (1997) 1219–1229.
[37] D.I. Papadimitriou, K.C. Giannakoglou, A continuous adjoint method with objective function derivatives based on boundary integrals, for inviscid and viscous flows, Comput. Fluids 36 (2) (2007) 325–341.
[38] D.I. Papadimitriou, K.C. Giannakoglou, Aerodynamic shape optimization using first and second order adjoint and direct approaches, Arch. Comput. Methods Eng. 15 (4) (2008) 447–488.
[39] D.I. Papadimitriou, K.C. Giannakoglou, Third-order sensitivity analysis for robust aerodynamic design using continuous adjoint, Int. J. Numer. Methods Fluids 71 (5) (2013) 652–670.
[40] D.I. Papadimitriou, C. Papadimitriou, Bayesian uncertainty quantification of turbulence models based on high-order adjoint, Comput. Fluids 120 (2015) 82–97.
[41] E.M. Papoutsis-Kiachagias, D.I. Papadimitriou, K.C. Giannakoglou, Robust design in aerodynamics using third-order sensitivity analysis based on discrete adjoint. Application to quasi-1D flows, Int. J. Numer. Methods Fluids 69 (3) (2012) 691–709.
[42] M.M. Putko, A.C. Taylor, P.A. Newman, L.L. Green, Approach for input uncertainty propagation and robust design in CFD using sensitivity derivatives, J. Fluids Eng. 124 (1) (2002) 60–69.
[43] J. Reuther, A. Jameson, J. Farmer, L. Martinelli, D. Saunders, Aerodynamic Shape Optimization of Complex Aircraft Configurations via an Adjoint Formulation, vol. 96, NASA Ames Research Center, Research Institute for Advanced Computer Science, 1996.
[44] P.L. Roe, Approximate Riemann solvers, parameter vectors, and difference schemes, J. Comput. Phys. 43 (2) (1981) 357–372.
[45] C. Schillings, S. Schmidt, V. Schulz, Efficient shape optimization for certain and uncertain aerodynamic design, Comput. Fluids 46 (1) (2011) 78–87.
[46] V. Schulz, C. Schillings, Problem formulations and treatment of uncertainties in aerodynamic design, AIAA J. 47 (3) (2009) 646–654.
[47] S.A. Smolyak, Quadrature and interpolation formulas for tensor products of certain classes of functions, Dokl. Akad. Nauk SSSR 4 (1963) 123.
[48] K. Svanberg, The method of moving asymptotes – a new method for structural optimization, Int. J. Numer. Methods Eng. 24 (2) (1987) 359–373.
[49] A.A. Taflanidis, J.L. Beck, Stochastic subset optimization for optimal reliability problems, Probab. Eng. Mech. 23 (2) (2008) 324–338.
[50] X. Wang, C. Hirsch, Z. Liu, S. Kang, C. Lacor, Uncertainty-based robust aerodynamic optimization of rotor blades, Int. J. Numer. Methods Eng. 94 (2) (2013) 111–127.
[51] D.W. Zingg, S. Elias, Aerodynamic optimization under a range of operating conditions, AIAA J. 44 (11) (2006) 2787–2792.